

Non-perturbative Renormalization of Bilinear Operators on Fine Lattice

Hwancheol Jeong, Weonjong Lee, Jeonghwan Pak, Sungwoo Park

*Lattice Gauge Theory Research Center, CTP, and FPRD,
Department of Physics and Astronomy,
Seoul National University, Seoul, 151-747, South Korea
E-mail: wlee@snu.ac.kr*

Jangho Kim*

*National Institute of Supercomputing and Networking,
Korea Institute of Science and Technology Information, Daejeon 34141, Korea
E-mail: jangho@kisti.re.kr*

SWME Collaboration

We present results of the wave function renormalization factor Z_q and mass renormalization factor Z_m obtained using non-perturbative renormalization (NPR) method in the RI-MOM scheme with HYP improved staggered quarks. We use fine ensembles of MILC asqtad lattices ($N_f = 2 + 1$) with $28^3 \times 96$ geometry, $a \approx 0.09$ fm, and $am_\ell/am_s = 0.0062/0.031$. We also study on scalability of Z_q and Z_m by comparing the results on the coarse and fine ensembles.

*The 33rd International Symposium on Lattice Field Theory
14 -18 July 2015
Kobe International Conference Center, Kobe, Japan*

*Speaker.

1. Introduction

In our previous work [1], we presented the results of the wave function renormalization factor Z_q , mass renormalization factor Z_m and the complete set of renormalization factors for bilinear operators obtained on the $20^3 \times 64$ MILC asqtad coarse lattice at $a \approx 0.12$ fm with $am_\ell/am_s = 0.01/0.05$. In this proceeding, we analyse the Z_q and Z_m on the $28^3 \times 96$ MILC asqtad fine lattices ($a \approx 0.09$ fm, $am_\ell/am_s = 0.0062/0.031$) and compare the results with those on the coarse lattices.

2. Results

We calculate the renormalization factors with Landau gauge fixing using HYP-smearred staggered quarks. To do the chiral extrapolation, we perform the measurements with 5 valence quark masses ($am = 0.0062, 0.0124, 0.0186, 0.0248, 0.031$) on the MILC fine ensembles at $a \approx 0.09$ fm. We also carry out the measurements for 20 external momenta given in Table 1. The measurements are done over 30 gauge configurations.

| $n(x, y, z, t)$ | $a \tilde{p} $ | GeV | $n(x, y, z, t)$ | $a \tilde{p} $ | GeV | $n(x, y, z, t)$ | $a \tilde{p} $ | GeV |
|-----------------|----------------|--------|-----------------|----------------|--------|-----------------|----------------|--------|
| (1, 1, 1, 3) | 0.4355 | 1.0197 | (1, 1, 1, 4) | 0.4686 | 1.0974 | (1, 2, 1, 4) | 0.6088 | 1.4257 |
| (1, 2, 1, 6) | 0.6755 | 1.5819 | (2, 1, 2, 6) | 0.7794 | 1.8250 | (2, 2, 2, 7) | 0.9023 | 2.1130 |
| (2, 2, 2, 8) | 0.9372 | 2.1947 | (2, 2, 2, 9) | 0.9753 | 2.2839 | (2, 3, 2, 7) | 1.0324 | 2.4177 |
| (2, 3, 2, 8) | 1.0631 | 2.4895 | (2, 3, 2, 9) | 1.0968 | 2.5684 | (3, 2, 3, 8) | 1.1756 | 2.7529 |
| (3, 3, 3, 7) | 1.2528 | 2.9337 | (3, 3, 3, 8) | 1.2782 | 2.9931 | (3, 3, 3, 10) | 1.3371 | 3.1312 |
| (3, 4, 3, 9) | 1.4349 | 3.3602 | (4, 3, 4, 10) | 1.5789 | 3.6973 | (4, 4, 4, 10) | 1.6868 | 3.9501 |
| (4, 4, 4, 12) | 1.7418 | 4.0788 | (4, 4, 4, 14) | 1.8046 | 4.2259 | | | |

Table 1: The list of momenta used for our analysis. The first column is the four vectors in the units of $(\frac{2\pi}{L_s}, \frac{2\pi}{L_s}, \frac{2\pi}{L_s}, \frac{2\pi}{L_t})$, where L_s (L_t) is the number of sites in the spatial (temporal) direction.

2.1 Wave Function Renormalization Factor Z_q

Let us consider the conserved vector current to obtain the wave function renormalization factor Z_q . We use the same method as in Ref. [1] to obtain the Z_q . First, we convert the raw data to the data defined at a common scale (CS) $\mu_0 = 3$ GeV using the four-loop RG evolution equation in Ref. [2, 3]. In Fig. 1, we present the raw data as the black circles and CS data as blue diamonds as a function of the square of reduced momentum $(a\tilde{p})^2$ at a fixed quark mass ($am = 0.0062$).

After converting the raw data to the CS data, we perform the fitting with respect to quark masses at a fixed external momentum to the following fitting function. We call this m-fit.

$$f_{\text{m-fit}} = b_1 + b_2 \cdot am + b_3 \cdot (am)^2 \quad (2.1)$$

The fitting results are presented in Table 2 and the plot is given in Fig. 2(a).

We take b_1 as the chiral limit values which are function of external momentum $(a\tilde{p})^2$. After m-fit, we fit b_1 to the following fitting function. We call this p-fit.

$$f_{\text{p-fit}} = c_1 + c_2(a\tilde{p})^2 + c_3 \cdot ((a\tilde{p})^2)^2 + c_4 \cdot (a\tilde{p})^4 \quad (2.2)$$

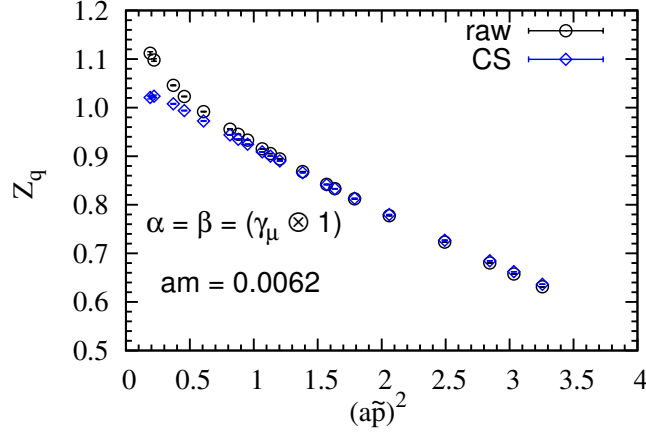


Figure 1: Z_q obtained from conserved vector current ($V \times S$) at a fixed quark mass ($am = 0.0062$). The black circles represent raw data and blue diamonds are CS data at a CS $\mu_0 = 3 \text{ GeV}$.

| b_1 | b_2 | b_3 | χ^2/dof |
|-------------|------------|-----------|---------------------|
| 0.84141(15) | 0.0153(97) | -0.31(17) | 0.004(10) |

Table 2: m-fit results for Z_q at $\mu_0 = 3 \text{ GeV}$ for a fixed external momentum $n = (3, 3, 3, 7)$.

| c_1 | c_2 | c_3 | c_4 | χ^2/dof |
|------------|-------------|-------------|------------|---------------------|
| 1.0567(11) | -0.1452(10) | 0.00294(14) | 0.0082(11) | 0.13(26) |

Table 3: P-fit results for Z_q at $\mu_0 = 3 \text{ GeV}$.

The fitting results are presented in Table 3 and the plot is presented in Fig. 2(b). The $\mathcal{O}((a\tilde{p})^2)$ and higher order terms correspond to lattice artifacts. Hence, we take c_1 as Z_q value in RI-MOM scheme at $\mu_0 = 3 \text{ GeV}$. Using the four-loop RG running formula [2, 3], we convert the Z_q from the RI-MOM scheme to the $\overline{\text{MS}}$ scheme.

We estimate the systematic error in two different ways. One systematic error comes from truncation of four-loop RG running factor which is used to convert the Z_q from the RI-MOM scheme to the $\overline{\text{MS}}$ scheme. Hence, we take five-loop uncertainty ($\sim \mathcal{O}(\alpha_s^4)$) and define E_t as follows.

$$E_t = Z_q^{\text{RI-MOM}} \cdot (\alpha_s)^4 \quad (2.3)$$

The other systematic error comes from the difference between the conserved vector and axial currents. Theoretically, Z_q obtained from the conserved vector and axial currents must be identical to each other. However, they are not same in our study. Hence, we take the difference of them as the systematic error and define E_Δ as follows.

$$E_\Delta = |Z_q(V \otimes S) - Z_q(A \otimes P)| \quad (2.4)$$

The total error (E_{tot}) is obtained adding the statistical error (E_{stat}) and the systematic errors in

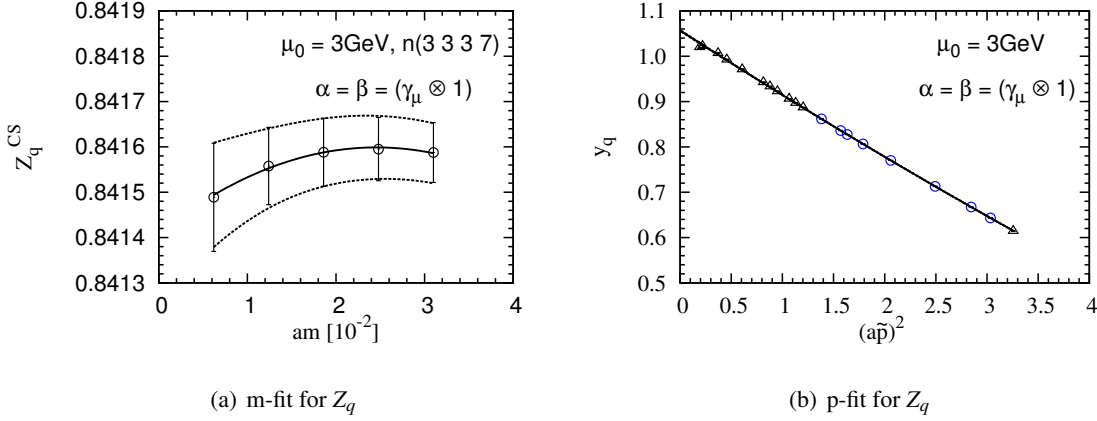


Figure 2: (a) m-fit results for Z_q at a reduced momentum $n = (3, 3, 3, 7)$ and (b) p-fit results for y_q . Here, we use the conserved vector current at $\mu_0 = 3\text{GeV}$. $y_q \equiv Z_q(\mu_0, am = 0) - \langle c_4 \rangle (a\tilde{p})^4$. The blue circles are used for fitting.

quadrature. We present the final result of Z_q in $\overline{\text{MS}}$ scheme at $\mu_0 = 3\text{GeV}$ and its statistical and systematic errors in Table 4.

| $Z_q^{\overline{\text{MS}}}(\mu_0)$ | E_{stat} | E_t | E_Δ | E_{tot} |
|-------------------------------------|-------------------|--------|------------|------------------|
| 1.0494 | 0.0011 | 0.0038 | 0.0099 | 0.0107 |

Table 4: Z_q in the $\overline{\text{MS}}$ scheme at $\mu_0 = 3\text{GeV}$ with statistical and systematic errors.

2.2 Quark Mass Renormalization Factor Z_m

Quark mass renormalization factor Z_m is obtained from the bilinear operator $[S \otimes S]$. Here, we use the same analysis method as in Ref. [1]. Note that we analyse $Z_q \cdot Z_m$ instead of Z_m directly. After we obtain the $Z_q \cdot Z_m$ in RI-MOM scheme at $\mu_0 = 3\text{GeV}$ through m-fit and p-fit, we divide by Z_q obtained from the conserved vector current. First, we convert raw data to the CS data using the four-loop RG running formula for $Z_q \cdot Z_m$. We present the raw and CS data for $Z_q \cdot Z_m$ in Fig. 3.

Using the CS data for $Z_q \cdot Z_m$, we carry out m-fit and p-fit. The fitting functions for m-fit and p-fit are

$$g_{\text{m-fit}} = d_1 + d_2 \cdot am + d_3 \cdot \frac{1}{(am)^2} \quad (2.5)$$

$$g_{\text{p-fit}} = h_1 + h_2(a\tilde{p})^2 + h_3 \cdot ((a\tilde{p})^2)^2 + h_4 \cdot (a\tilde{p})^4. \quad (2.6)$$

We present fitting results of m-fit in Table 5 and in Fig. 4 (a). We show fitting results of p-fit in Table 6 and in Fig. 4 (b).

We determine Z_m by dividing $Z_q \cdot Z_m$ by Z_q obtained using the conserved vector current. Then, we convert Z_m in the RI-MOM scheme into that in the $\overline{\text{MS}}$ scheme using the four-loop RG evolution formula.

$$Z_m^{\overline{\text{MS}}}(\mu_0) = U(\infty \rightarrow \mu_0, \overline{\text{MS}}) U(\mu_0 \rightarrow \infty, \text{RI-MOM}) Z_m^{\text{RI-MOM}}(\mu_0), \quad (2.7)$$

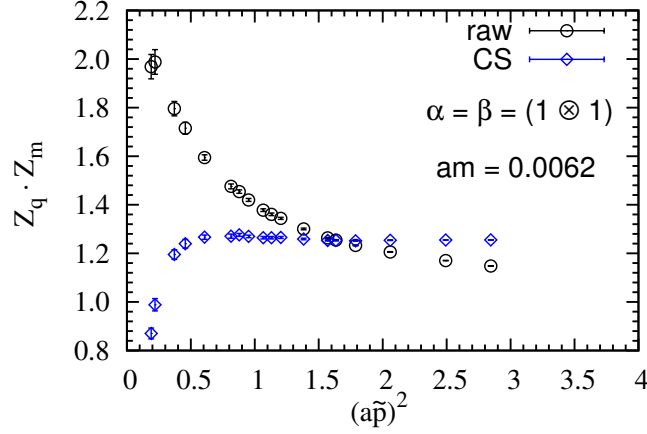


Figure 3: $Z_q \cdot Z_m$ obtained from $[S \times S]$ bilinear operator at $am = 0.0062$. Here, $\mu_0 = 3$ GeV.

| d_1 | d_2 | d_3 | χ^2/dof |
|-------------|------------|------------------|---------------------|
| 1.25664(60) | -0.354(15) | -0.000000019(51) | 0.017(25) |

Table 5: Fitting results of $Z_q \cdot Z_m$ for m-fit. The reduced momentum is fixed to $n = (3, 4, 3, 9)$.

| h_1 | h_2 | h_3 | h_4 | χ^2/dof |
|------------|-------------|-------------|------------|---------------------|
| 1.3069(39) | -0.0459(35) | 0.00191(62) | 0.0308(45) | 0.37(32) |

Table 6: Fitting results of $Z_q \cdot Z_m$ for p-fit.

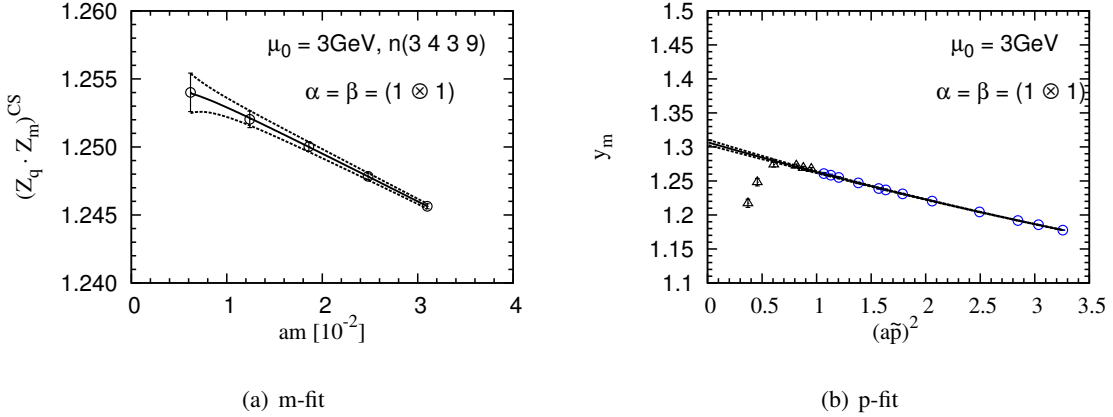
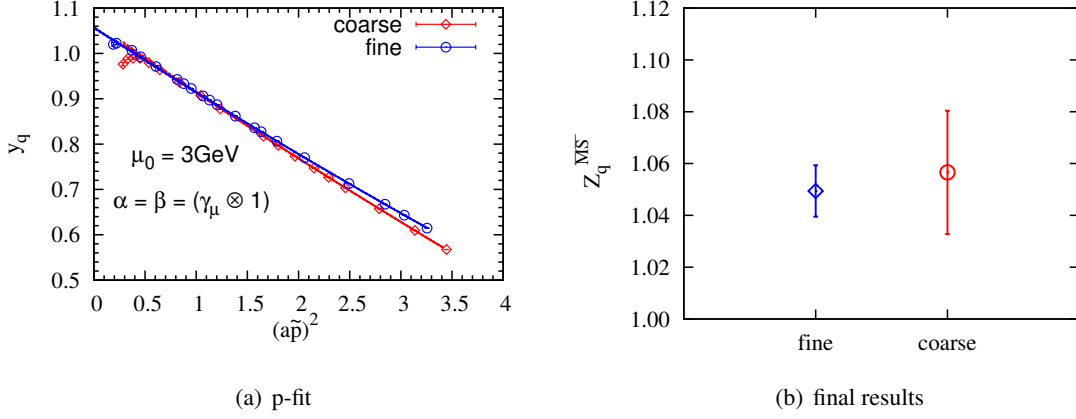


Figure 4: Fitting results of $Z_q \cdot Z_m$ for (a) m-fit and (b) p-fit. For the m-fit, the reduced momentum is fixed to $n = (3, 4, 3, 9)$. For the p-fit, $y_m \equiv (Z_q \cdot Z_m)(\mu_0, am = 0) - \langle h_4 \rangle (a\tilde{p})^4$. The blue circle data are used for fitting.

where $U(\mu_1 \rightarrow \mu_2, R)$ is the RG evolution matrix from the scale μ_1 to μ_2 in the R scheme. The results are summarized in Table 7. Here, the systematic errors are estimated in the same way as in Z_q .

| $Z_m^{\overline{\text{MS}}}(\mu_0)$ | E_{stat} | E_t | E_Δ | E_{tot} |
|-------------------------------------|------------|--------|------------|-----------|
| 1.0117 | 0.0032 | 0.0044 | 0.0005 | 0.0055 |

Table 7: Z_m in $\overline{\text{MS}}$ scheme at $\mu_0 = 3 \text{ GeV}$.**Figure 5:** Comparison of $Z_q(\mu_0)$ on the coarse and fine lattices. The red (blue) data represent results on the coarse (fine) lattice.

2.3 Comparison of Z_q and Z_m between coarse and fine lattices

Now, we present the comparison of the Z_q and Z_m results at $\mu_0 = 3 \text{ GeV}$ between coarse and fine lattices in Fig. 5 and Fig. 6.

The results of Z_q and Z_m at $\mu_0 = 3 \text{ GeV}$ on coarse and fine lattices are presented in Table 8. We find that the total errors of $Z_q^{\overline{\text{MS}}}$ and $Z_m^{\overline{\text{MS}}}$ on fine lattice are reduced dramatically compared with those of coarse lattice.

| | coarse | fine |
|---|-----------------|----------------|
| $Z_q^{\overline{\text{MS}}}(3\text{GeV})$ | 1.0566(59)(231) | 1.0494(11)(99) |
| $Z_m^{\overline{\text{MS}}}(3\text{GeV})$ | 0.865(21)(25) | 1.0117(32)(44) |

Table 8: The comparison of Z_q and Z_m at $\mu_0 = 3 \text{ GeV}$ between coarse and fine lattices. The first error is statistical and the second is systematic.

3. Conclusion

Here, we present the results of the wave function renormalization factor Z_q and mass renormalization factor Z_m for the staggered bilinear operators defined in the $\overline{\text{MS}}$ scheme at $\mu_0 = 3 \text{ GeV}$. We use the NPR method in the RI-MOM scheme as an intermediate scheme. We use one of the MILC asqtad fine ($a \approx 0.09 \text{ fm}$) ensembles to calculate the matching factors. By comparing results with those on the coarse ensembles, we find that the statistical and systematic errors of Z_q and Z_m are reduced dramatically on the fine lattice. We plan to extend the calculation to the superfine ($a \approx 0.06 \text{ fm}$) and ultrafine ($a \approx 0.045 \text{ fm}$) ensembles in the future. As a consequence, we will

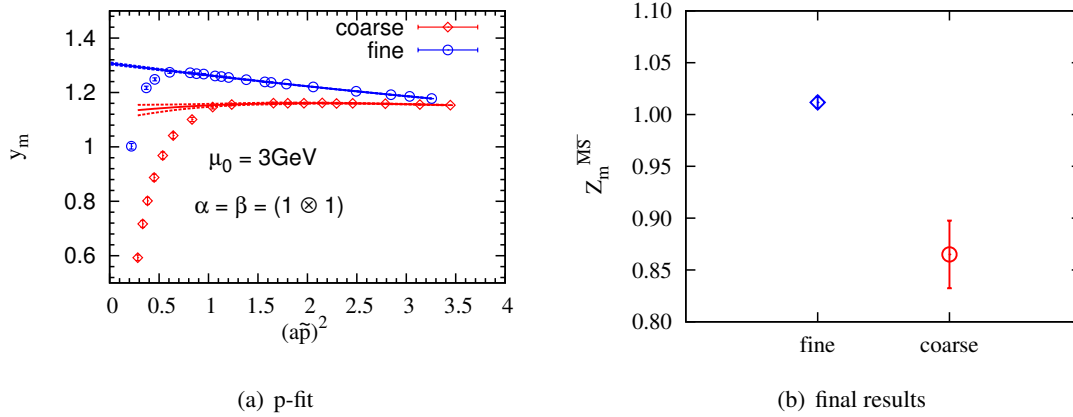


Figure 6: Comparison of $Z_m(\mu_0)$ on the coarse and fine lattices. The red (blue) data represent results on the coarse (fine) lattice.

study on the scalability of Z_q and Z_m . We also plan to calculate the renormalization factors on the fine ensembles with different sea quark masses, which will help us to understand their dependence on sea quark masses.

Acknowledgments

J. Kim is supported by Young Scientists Fellowship through National Research Council of Science & Technology (NST) of KOREA. The research of W. Lee is supported by the Creative Research Initiatives Program (No. 2015001776) of the NRF grant funded by the Korean government (MEST). W. Lee would like to acknowledge the support from the KISTI supercomputing center through the strategic support program for the supercomputing application research (No. KSC-2014-G3-002) with much gratitude. Computations were carried out on the DAVID GPU clusters at Seoul National University.

References

- [1] J. Kim, J. Kim, W. Lee, and B. Yoon *PoS LATTICE2013* (2013) 308, [[1310.4269](#)].
- [2] K. Chetyrkin and A. Retey, *Renormalization and running of quark mass and field in the regularization invariant and \overline{MS} schemes at three loops and four loops*, *Nucl.Phys.* **B583** (2000) 3–34, [[hep-ph/9910332](#)].
- [3] Y. Aoki, P. Boyle, N. Christ, C. Dawson, M. Donnellan, *et al.* *Phys.Rev.* **D78** (2008) 054510, [[0712.1061](#)].